

This article was downloaded by:

On: 28 January 2011

Access details: *Access Details: Free Access*

Publisher *Taylor & Francis*

Informa Ltd Registered in England and Wales Registered Number: 1072954 Registered office: Mortimer House, 37-41 Mortimer Street, London W1T 3JH, UK



## Physics and Chemistry of Liquids

Publication details, including instructions for authors and subscription information:

<http://www.informaworld.com/smpp/title~content=t713646857>

### On the Relation Between the Effective Pair-potential and the Static Structure Factor in Liquid Metals

L. G. Olsson<sup>a</sup>; U. Dahlborg<sup>a</sup>

<sup>a</sup> Institute for Reactorphysics, Royal Institute of Technology, Stockholm, Sweden

**To cite this Article** Olsson, L. G. and Dahlborg, U.(1982) 'On the Relation Between the Effective Pair-potential and the Static Structure Factor in Liquid Metals', *Physics and Chemistry of Liquids*, 11: 3, 225 – 240

**To link to this Article:** DOI: 10.1080/00319108208080745

**URL:** <http://dx.doi.org/10.1080/00319108208080745>

PLEASE SCROLL DOWN FOR ARTICLE

Full terms and conditions of use: <http://www.informaworld.com/terms-and-conditions-of-access.pdf>

This article may be used for research, teaching and private study purposes. Any substantial or systematic reproduction, re-distribution, re-selling, loan or sub-licensing, systematic supply or distribution in any form to anyone is expressly forbidden.

The publisher does not give any warranty express or implied or make any representation that the contents will be complete or accurate or up to date. The accuracy of any instructions, formulae and drug doses should be independently verified with primary sources. The publisher shall not be liable for any loss, actions, claims, proceedings, demand or costs or damages whatsoever or howsoever caused arising directly or indirectly in connection with or arising out of the use of this material.

# On the Relation Between the Effective Pair-potential and the Static Structure Factor in Liquid Metals

L. G. OLSSON and U. DAHLBORG

*Institute for Reactorphysics, Royal Institute of Technology, S-10044 Stockholm, Sweden.*

*(Received May 20, 1981)*

Accurate neutron diffraction measurements of the static structure factor  $S(Q)$  for small wavevector transfers  $Q$  have been used to obtain the “coarse” structure of the long-range part of the effective inter-particle potential in liquid aluminium, lead and bismuth. An extended version of the random phase approximation developed by Gaskell has been used. It is found that for Al and Pb the potential is of simple oscillatory nature while for Bi it is of ledge type. Finer details of the shape of the potential could not be evaluated. Methods to determine a good pair-potential by combining experimental results and molecular dynamics calculations are suggested.

## I INTRODUCTION

For wavevector transfers  $Q > Q_m$ , where  $Q_m$  is the position of the principal maximum of the structure factor  $S(Q)$ , the density fluctuations in a liquid are almost entirely caused by “excluded volume effects.” It is therefore reasonable to assume that  $S(Q)$  in this  $Q$ -range is essentially governed by repulsive forces of short range. For smaller  $Q$ -values, particularly when  $Q$  tends to zero, it is on the other hand expected that the attractive forces between the particles are of increasing importance, although the effect of the repulsive ones cannot be neglected. Thorough molecular dynamics (MD) calculations by Hansen and Schiff,<sup>1</sup> applying various repulsive inter-particle potentials, clearly indicate the importance of the repulsive forces on  $S(Q)$  even at small  $Q$ . Thus, the isothermal compressibility, proportional to  $S(0)$ , will depend on both the attractive and repulsive parts of the pair-potential.

Several different schemes, all approximate to some degree, exist in order to extract an effective inter-particle potential from a measured  $S(Q)$ . For a review of these we refer to the excellent article by Barker and Henderson.<sup>2</sup> Recently Rosenfeld and Ashcroft<sup>3</sup> suggested to use a modified hypernetted chain equation where the only free parameter can be determined by imposing thermodynamic consistency. Common to all these methods is that  $S(Q)$  over the full  $Q$ -range has to be used. In this report we will restrict ourselves to the region of small  $Q$ , thus, according to the discussion above, aiming mainly at a better understanding of the long range forces in a molecular system. Two different theories are then available, one developed by Gaskell<sup>4</sup> and one by Evans and Schirmacher.<sup>5</sup> Both represent a generalization of the random phase approximation (RPA). However, from numerical reasons and also due to the fact that it has not been tested against experimental data we have only tried the one obtained by Gaskell.

During the recent years accurate measurements of  $S(Q)$  for  $Q$  in the range of 0.15 to 1.0  $\text{\AA}^{-1}$  have been performed for liquid Al, Pb and Bi.<sup>6</sup> In order to use these data for our purpose we have thus utilized the improved random phase approximation by Gaskell.<sup>4</sup> In this theory a pair-potential,  $v(r)$ , is assumed to describe the effective interaction between the particles. As in the RPA the potential is divided in two parts:

$$v(r) = v_0(r) + v_1(r) \quad (1)$$

where  $v_0(r)$  denotes the repulsive or short-range part and  $v_1(r)$  the corresponding perturbation or long-range part;  $r$  is the distance from the particle to the origin. Compared to the ordinary RPA, valid for  $Q \ll Q_m$ , Gaskell includes correlation effects manifesting themselves as an extra term in the analytical expression of the RPA. This correction can be considered as an extension of the  $Q$ -range for the validity of the RPA as well as a check of the RPA itself. One ambiguity arises, however, when the pair-potential is divided in two parts as in Eq. (1). The division is quite arbitrary and it cannot be tacitly assumed that  $v_1(r)$  is vanishing inside the range of  $\sigma$  of the repulsive forces. The effect on this of  $S(Q)$  must in some way be tested for each tried form of  $[v_1(r)]_{r>\sigma}$ .

Another uncertainty which has to be taken into account is the hardness of the core. In order to make an analysis meaningful the main character of  $v_0(r)$  must be known at least in terms of being of hard or soft repulsive nature. The structure factors  $S_0(Q)$ , based on pure repulsive potentials  $v_0(r) \sim r^{-n}$ , do not differ very much and describe the experimental  $S(Q)$  for simple "hard" systems like Al and Pb reasonable well if  $Q > Q_m/2$  and  $n \gg 1$ . For instance, according to the MD calculations by Hansen and Schiff<sup>1</sup> the principal maximum for a hard-core system as well as a system of particles governed by a  $r^{-9}$ -potential agree both within 10% with measured

data (with exception of the more complex liquids as Ga and Bi). The corresponding situation holds for "soft" systems like liquid Na and Rb ( $n \sim 4$ ). It should be mentioned that there is also a minor phase shift of the oscillations of the calculated and measured structure factors. This is, however, supposed to be caused by the omission of attractive forces in the MD studies. It is on the other hand interesting to note that for  $Q < Q_m/2$  the structure factors  $S_0(Q)$  differ clearly for different  $v_0(r)$  and discrepancies of the order of 100% between the computed (MD) and measured data frequently occur.

In spite of these difficulties, it should be possible to obtain empirical information about the attractive forces (or  $v_1(r)$ ) by restricting the comparison of the calculated and measured  $S(Q)$  to small  $Q$ , if we also include the hardness of the reference system as a variable. In the present studies of liquid Al, Pb and Bi we have thus chosen  $n$  to be in the range  $6 \leq n \leq \infty$ . In Section II of this report the basic formulas and the numerical methods used to analyse the structure factors are briefly described. The results are compiled graphically in Section III and discussed in some detail. The conclusions are finally summarized in Section IV.

## II BASIC FORMULAS AND NUMERICAL METHOD

The structure factor according to the improved RPA by Gaskell<sup>4</sup> can be expressed in the following way

$$\frac{1}{S(Q)} = \sum_{i=0}^2 \frac{1}{S_i(Q)} \quad (2a)$$

where  $S(Q)$  and  $S_0(Q)$  thus are the structure factors for the real and reference systems, respectively, and  $Q$  the wavevector transfer in the scattering process. The remaining terms are defined by the relations

$$\frac{1}{S_1(Q)} = \frac{1}{4\pi Q\rho} \int_0^\infty v_1^*(r)r \sin(Qr) dr \quad (2b)$$

$$\frac{1}{S_2(Q)} = \frac{1}{\rho(2\pi)^2} \int_0^\infty \int_{-1}^1 S_0^2(k) \frac{S_0(a) - 1}{S_1(k)} k^2 dk d\mu \quad (2c)$$

$$a = (Q^2 + k^2 + 2kQ\mu)^{1/2} \quad (2d)$$

$\rho$  is the number density of the system and  $\mu$  the cosine for the angle between the  $Q$  and  $k$  vectors.  $v_1^*(r) = v_1(r)/k_B T$  is the perturbation potential that should be assigned the repulsive potential  $v_0^*(r)$ , also in units of  $k_B T$  (compare Eq. (1));  $k_B$  and  $T$  have their usual meanings. In order to arrive at any

results applying Eq. (2) it is convenient to assume analytical expressions for  $v_1^*(r)$  making it possible to numerically evaluate the Fourier transform (Eq. (2b)) and the integral (Eq. (2c)). A rather elaborate expressions containing 6 adjustable parameters was chosen in the present studies. It consists of a sum of a differentiated Gaussian function with a weight function displaceable along the  $r$ -axis and an exponential function. Such a combination of analytical expressions allow very different shapes of  $v_1^*(r)$ , from a one-period oscillating function to a simple exponential one. It is thus assumed that all kinds of oscillations of larger periodicity are damped out (further discussed below).

Thus the following expressions were used to describe  $v_1^*(r)$  for  $r \geq \sigma$ :

$$v_1^*(r) = w(r) \cdot \exp[-C_3(r - r_0)^2] + \frac{C_4 \cdot \exp(-C_6 r)}{r}$$

$$w(r) = C_2 \cdot \exp[-C_1(r - C_5)^2] \left(\frac{r}{r_0}\right)^m (r - r_0)$$

$$r_0 = \sigma + (2C_3)^{-1/2} \quad (3a)$$

and for  $r < \sigma$ :

$$v_1^*(r) = 0 \quad (\text{type I potential})$$

$$v_1^*(r) = [v_1^*(\sigma)]_{r \geq \sigma} \quad (\text{type II potential}) \quad (3b)$$

Due to the ambiguity of the definition of the perturbation potential for  $r < \sigma$  ( $\sigma$  is the effective hard-core diameter ascribed to the particles) two limiting cases have been considered for each tried reference system (compare Section I). Furthermore, the exponent  $m$  was always put equal to 0 for the type I potential and 2 for the type II case. For reference systems we used the hard-core system<sup>7</sup> and the MD results by Hansen and Schiff<sup>1</sup> for the  $r^{-12}$ —and  $r^{-6}$ —potentials. It should also be mentioned that the MD results were obtained at a number density  $\rho_0$  corresponding to the crystallization point. The correction to the number density of the real system,  $\rho$ , was performed in the following way:

$$S_{\text{MD}}(Q, \rho) = S_{\text{MD}}(Q, \rho_0) \cdot \left[ \frac{S(Q, \rho)}{S(Q, \rho_0)} \right]_{\text{hc}} \quad (4)$$

where the subscripts MD and hc refer to the molecular dynamics and the hard-core results, respectively. This density correction is quite arbitrary and may be justified as long as the ratio calculated on basis of the hard-core system appears to be close to 1.

### III RESULTS AND DISCUSSION

#### A. Basic Properties of the Method for Analysis

The structure factor  $S(Q)$  according to Eq. (2) was calculated using the expressions in Eq. (3) for the perturbation potential  $v_1^*(r)$  and a fixed reference system  $S_0(Q)$ . Some test calculations were performed on a hard-core system, but the results of these should also be relevant for other types of reference systems. The aim was to study the numerical stability and the features of  $S(Q)$  due to changes in  $v_1^*(r)$ . The calculations were carried through with the parameters  $C_i$ ,  $i = 1, \dots, 6$ , chosen to give widely different shapes of  $v_1^*(r)$  without any physical meaning. Extra terms of oscillating character (not accounted for in Eq. (3)) were also added in order to investigate the effects of the rapid truncation of  $v_1^*(r)$  and a superimposed "fine-structure" on  $v_1^*(r)$ , respectively. The results are compiled in Figure 1. The hard-core diameter  $\sigma$  was put equal to 2.59 Å, i.e. the value appropriate for liquid Al. The analytical forms available from Eq. (3) are subsequently also referred to as the "coarse structure" of the perturbation potential.

In Figure 1A the effects on  $S(Q)$  of two opposite shapes of the coarse structure of  $v_1^*(r)$  are shown. If  $v_1^*(r)$  is made positive and monotonically decreasing the corresponding  $S(Q)$  at small  $Q$  falls below  $S_0(Q)$  for the reference system. If, on the other hand,  $v_1^*(r)$  in a similar way is made negative  $S(Q)$  exceeds  $S_0(Q)$  for small  $Q$ . The latter result is in agreement with the sticky hard-sphere model,<sup>8</sup> which prescribes a considerable increase of the compressibility compared to the pure hard-core model. The discrepancies between  $S(Q)$  and  $S_0(Q)$  in these two extreme cases are very large. In practice some kind of an oscillatory behaviour of  $v_1^*(r)$  is more likely for liquid metals and the deviations from  $S_0(Q)$  smaller.

In Figure 1B we show some results from the numerical tests with respect to the fine-structure and truncation of  $v_1^*(r)$ . A given  $v_1^*(r)$  (solid line) was modified to give the curves denoted by the dash-dotted and dotted lines. The calculations were carried through with the imposed condition that  $S(Q)$  should not change more than about 10% which is a realistic error of a measured  $S(Q)$  in this  $Q$ -region. It is seen that a fairly large modification of  $v_1^*(r)$  can be allowed, if it occurs close to the minimum of the potential. If, however, an oscillation is still persisting at large  $r$  its amplitude must be made very small otherwise  $S(Q)$  will obtain unrealistic values. It is possible that a  $r$ -dependent period of the oscillations could allow a larger amplitude but in such a case the periodicity must be known in great detail. Therefore such types of oscillations, including the Friedel ones, in  $v_1^*(r)$  besides the coarse structure are omitted in the subsequent analysis. It should also be mentioned that the small deviations in  $S(Q)$ , due to the previously discussed modifications of  $v_1^*(r)$ , could easily be fully compensated for by minor changes

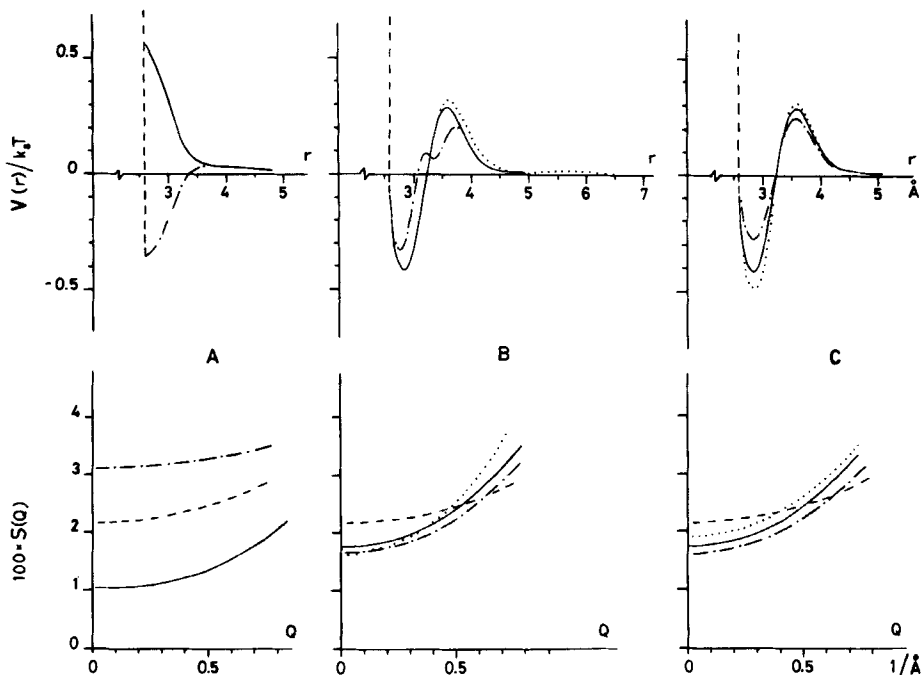


FIGURE 1 The main features and the numerical stability of the computer routines based on Gaskell's theory.<sup>4</sup> The reference system, a hard-core system (broken lines), is kept fixed while the perturbation potential is varied. Upper plots give the tried potentials and the lower ones the corresponding structure factors. All the denotations are mutually connected. (A) The main characteristics due to a very simple form of the perturbation are shown for two opposite cases. (B) The effects of additional oscillations to a given shape of the perturbation potential (solid lines). (C) The impact on the structure factor caused by variation of the amplitude of the perturbation potential. The calculation is restricted to a one-period oscillatory potential (see the text).

of the parameters  $C_i$  in the original expression of  $v_1^*(r)$ , Eq. (3). In Figure 1C, finally, the effects of amplitude changes of a given coarse potential shape are studied. A perturbation  $v_1^*(r)$  nearly symmetric around the  $r$ -axis was selected. It is demonstrated that large changes of  $v_1^*(r)$  cause only modest variations in  $S(Q)$  at small  $Q$ . It is probable that such discrepancies can be compensated for to give the same small  $Q$  values of  $S(Q)$  by combining the different perturbations with a reference system  $S_0(Q)$  somewhat modified, but still with the characterization hard,  $n > 6$  (or soft if such a system is studied).

The test calculations thus indicate that the adopted method of analysis (Section II) can only provide a first approximation of the coarse structure of the perturbation potential  $v_1^*(r)$ . Fine-structure effects superimposed on

$v_1^*(r)$  can be compensated for to give a correct  $S(Q)$  at small  $Q$ , a modified reference system  $S_0(Q)$  allows changes of the amplitude of  $v_1^*(r)$  as large as 25%, etc. In the present investigations we have therefore concentrated our efforts to establish some *limiting shapes* of  $v_1^*(r)$  with respect to  $S_0(Q)$  and the ambiguity of the perturbation potentials at small  $r$ . The parameters  $C_i$  in Eq. (3) are in the following determined by a least-square fitting procedure utilizing  $S(Q)$  according to Eq. (2) and experimental data contrary to the previous test calculations.

### B. The Effects of Various Reference Systems

Remembering the lack of uniqueness between  $S(Q)$  and  $v_1^*(r)$  discussed above, the effect on  $v_1^*(r)$  caused by using different reference systems  $S_0(Q)$  has to be investigated in more detail. It is expected that the repulsive forces in liquid Al, Pb and Bi are relatively hard implying that a pure hard-core system and the MD data for a  $r^{-12}$  and a  $r^{-6}$ -potential<sup>1</sup> were tried. For each case both the type I and II approximations were included in the calculations (Section II). The measured  $S(Q)$ , utilizing the neutron scattering technique,<sup>6</sup> cover the  $Q$ -range 0.19 to  $1.5 \text{ \AA}^{-1}$ . The final results are given in Tables I-III. The data have been thoroughly corrected for all instrumental effects as well as the multiple scattering contamination. The temperatures, at which the experiments were carried through, were chosen a few tens of degrees higher than the corresponding melting points, i.e. 705, 350 and 305°C for Al, Pb and Bi, respectively. Furthermore, for  $Q < 0.8 \text{ \AA}^{-1}$  the measured  $S(Q)$  could be reproduced by a parabolic function, the parameters of which were evaluated by means of least-square fit procedures (Table IV). The final comparison of the measured and calculated data was carried through utilizing this parabolic function plus  $S(0)$  calculated from the compressibility values according to ultra-sound measurements.<sup>9</sup> There is a range  $0 < Q < 0.19$

TABLE I  
Measured  $S(Q)$  for liquid aluminium at 705°C

$Q$	$S(Q)$	$Q$	$S(Q)$	$Q$	$S(Q)$
0.208	$0.019 \pm 6$	0.616	$0.029 \pm 3$	1.022	$0.055 \pm 4$
0.254	$0.022 \pm 5$	0.661	$0.031 \pm 3$	1.068	$0.062 \pm 4$
0.299	$0.021 \pm 5$	0.706	$0.030 \pm 4$	1.113	$0.059 \pm 4$
0.344	$0.024 \pm 4$	0.752	$0.039 \pm 4$	1.158	$0.060 \pm 4$
0.390	$0.025 \pm 4$	0.797	$0.041 \pm 4$	1.203	$0.069 \pm 4$
0.435	$0.021 \pm 4$	0.842	$0.046 \pm 4$	1.248	$0.065 \pm 4$
0.480	$0.022 \pm 4$	0.887	$0.044 \pm 4$	1.293	$0.069 \pm 4$
0.525	$0.026 \pm 4$	0.932	$0.054 \pm 4$	1.338	$0.071 \pm 4$
0.571	$0.022 \pm 4$	0.977	$0.052 \pm 4$		



TABLE II  
Measured  $S(Q)$  for liquid lead at 350°C

$Q$	$S(Q)$	$Q$	$S(Q)$	$Q$	$S(Q)$
0.190	0.007 ± 2	0.652	0.022 ± 2	1.113	0.047 ± 3
0.217	0.011 ± 2	0.679	0.024 ± 2	1.140	0.058 ± 3
0.245	0.012 ± 2	0.706	0.023 ± 2	1.167	0.059 ± 3
0.272	0.013 ± 2	0.733	0.027 ± 2	1.194	0.055 ± 3
0.299	0.012 ± 2	0.761	0.025 ± 2	1.221	0.057 ± 3
0.326	0.012 ± 2	0.788	0.029 ± 2	1.248	0.063 ± 3
0.353	0.013 ± 2	0.815	0.032 ± 2	1.275	0.070 ± 3
0.381	0.018 ± 2	0.842	0.031 ± 2	1.302	0.070 ± 3
0.408	0.014 ± 2	0.869	0.033 ± 2	1.329	0.072 ± 3
0.435	0.016 ± 2	0.896	0.030 ± 2	1.356	0.078 ± 3
0.462	0.016 ± 2	0.923	0.034 ± 2	1.383	0.078 ± 3
0.489	0.016 ± 2	0.950	0.034 ± 2	1.409	0.088 ± 3
0.516	0.016 ± 2	0.977	0.034 ± 2	1.436	0.096 ± 4
0.544	0.019 ± 2	1.004	0.038 ± 2	1.463	0.097 ± 4
0.571	0.019 ± 2	1.031	0.045 ± 2	1.490	0.105 ± 3
0.598	0.022 ± 2	1.059	0.045 ± 3		
0.625	0.027 ± 2	1.086	0.051 ± 3		

TABLE III  
Measured  $S(Q)$  for liquid bismuth at 305°C

$Q$	$S(Q)$	$Q$	$S(Q)$	$Q$	$S(Q)$
0.200	0.015 ± 5	0.650	0.019 ± 3	1.100	0.050 ± 4
0.245	0.008 ± 4	0.695	0.024 ± 4	1.145	0.052 ± 4
0.290	0.010 ± 4	0.740	0.027 ± 4	1.190	0.061 ± 4
0.335	0.012 ± 4	0.785	0.021 ± 4	1.235	0.066 ± 4
0.380	0.010 ± 4	0.830	0.025 ± 4	1.280	0.071 ± 4
0.425	0.011 ± 4	0.875	0.026 ± 4	1.325	0.082 ± 4
0.470	0.017 ± 4	0.920	0.037 ± 5	1.370	0.101 ± 4
0.515	0.014 ± 3	0.965	0.049 ± 4	1.415	0.117 ± 4
0.560	0.015 ± 3	1.010	0.043 ± 4	1.460	0.139 ± 5
0.605	0.020 ± 3	1.055	0.048 ± 4		

$\text{\AA}^{-1}$ , where experimental data are missing but we believe that this is of little importance in the present analysis. It should also be mentioned that no clear minima in the least-square fits were indicated during the computer runs to evaluate  $C_i$ ,  $i = 1, \dots, 6$ . This may be due to the parameters  $C_i$  not being linearly independent and/or the lack of uniqueness between  $S(Q)$  and  $v_i^*(r)$ . After about 15 iterations the parameters tended to oscillate around certain average values.

Before the results concerning the region of small  $Q$  are discussed it might be pertinent to show how well the selected reference systems  $S_0(Q)$  in general

TABLE IV

Parameters used to describe the hard-core reference systems and the experimental  $S(Q) = a_0 + a_1 Q^2$

Substance	Temp.  K	Density  atoms/Å <sup>3</sup>	Hard-core diameter  Å	$a_0$	$a_1$
Al	705	0.0527	2.59	0.0179 ± 0.0017	0.030 ± 0.002
Pb	350	0.0310	3.12	0.0091 ± 0.0013	0.030 ± 0.002
Bi	305	0.0280	3.00	0.0091 ± 0.0028	0.030 ± 0.002
Bi	305	0.0280	3.23, 2.45 <sup>a</sup>	0.0091 ± 0.0028	0.030 ± 0.002

<sup>a</sup> Refers to the double-shell system.

TABLE V

Position ( $Q_m$ ) and height of main peak of experimental  $S(Q)$  and of the  $S(Q)$  calculated by Hansen and Schiff<sup>1</sup> for repulsive potentials  $v(r) \sim r^{-n}$

		$Q_m$	$S(Q_m)$
Experimental data	Al	2.68 <sup>a</sup>	2.48 <sup>a</sup>
	Pb	2.21 <sup>b</sup>	2.75 <sup>b</sup>
	Bi	2.08 <sup>c</sup>	1.90 <sup>c</sup>
$n = \infty$	Al	2.68	2.70
	Pb	2.24	2.88
	Bi	2.21, 2.10 <sup>d</sup>	1.95, 1.95 <sup>d</sup>
$n = 12$	Al	2.72	2.53
	Pb	2.26	2.72
	Bi	—	—
$n = 6$	Al	2.70	2.48
	Pb	2.24	2.66
	Bi	—	—

<sup>a</sup> Ref. 10.

<sup>b</sup> Ref. 11.

<sup>c</sup> Ref. 12.

<sup>d</sup> Ref. 13.

reproduce the measured  $S(Q)$  for larger  $Q$ -values, considering the fact that no attractive forces are present in the calculated data. In Table V the positions and intensities of the principal maxima of  $S_0(Q)$  and  $S(Q)$  are tabulated together with other relevant information about the three systems. It is also seen that for liquid Bi simple reference systems, like the hard-core model, reproduces the experimental  $S(Q)$  rather bad, which could perhaps be expected because of the complexity of the electronic structure of Bi. The

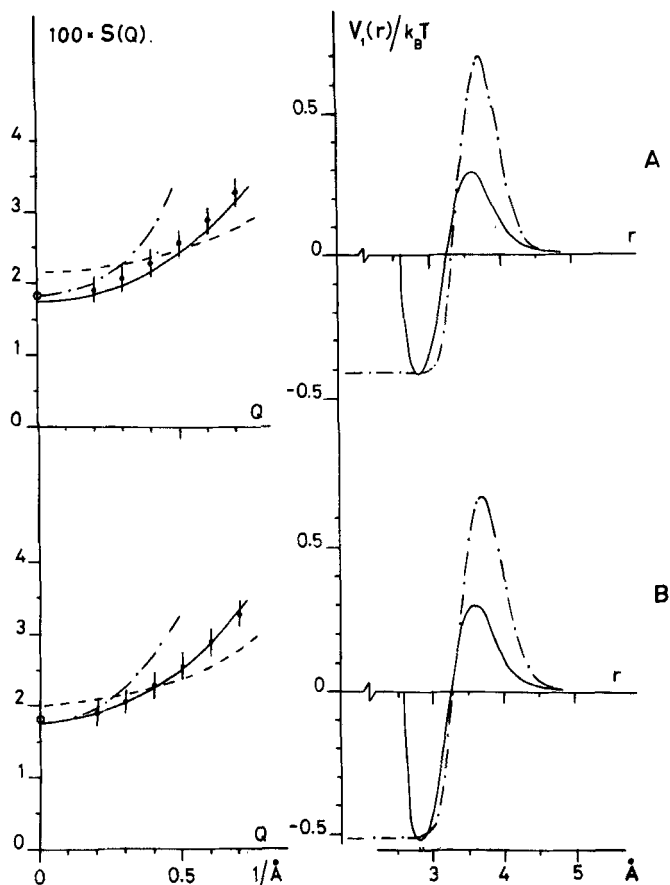


FIGURE 2 The perturbation potential  $v_1^*(r) = v_1(r)/k_B T$  and the corresponding structure factor  $S(Q)$  for liquid Al at 705°C. (A)  $S(Q)$  for a hard-core system (broken lines) and the corresponding results using Gaskell's theory. Solid lines denote the type I and dash-dotted lines the type II potential. The experimental data are given by the dots (neutron scattering)<sup>6</sup> and the circle (ultrasound).<sup>9</sup> (B) The same results for a reference system based on a repulsive pair-potential of  $r^{-12}$ -type.<sup>1</sup>

final results for  $v_1^*(r)$  and the corresponding  $S(Q)$  for  $Q < 0.5 \text{ \AA}^{-1}$  are shown in Figures 2, 3 and 4 for liquid Al, Pb and Bi, respectively.

In the case of Al and Pb the hard-core results are plotted in Figure A, solid lines for type I potential and dash-dotted in the case of type II potential. The ones based on a  $r^{-12}$  repulsive potential are shown in Figure B with the same notations. The results concerning the  $r^{-6}$ -potential are excluded, because the only difference from the  $r^{-12}$ -case is that the positive amplitude of  $v_1^*(r)$  is somewhat smaller. In all plots  $S_0(Q)$  is reproduced by a broken

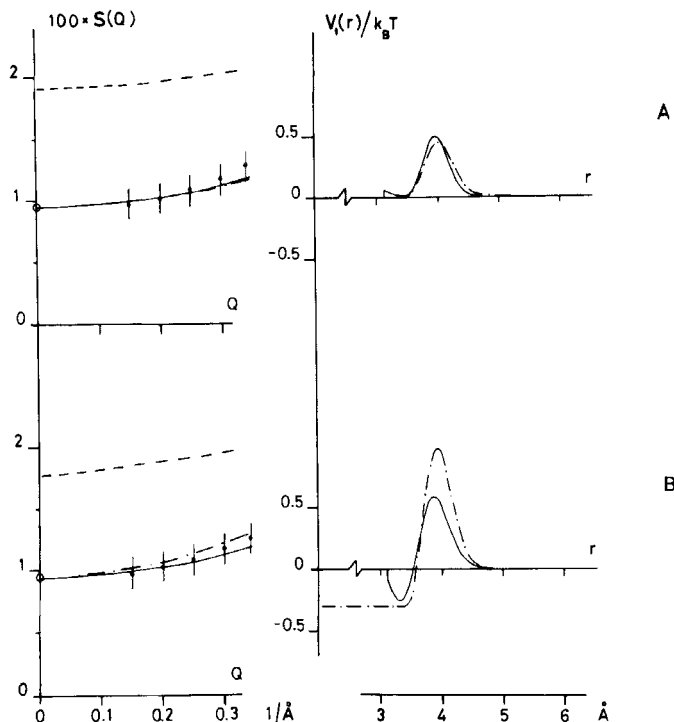


FIGURE 3 The perturbation potentials  $v_1^*(r)$  and the corresponding  $S(Q)$  for liquid Pb at 350°C for a hard-core system, Figures 3A, and a reference system based on a  $r^{-12}$ -potential, Figures 3B. All the denotations are the same as in Figures 2.

line. For Pb it is clear that  $S_0(Q)$  for the hard-core system overrides the measured  $S(Q)$  for  $Q < 0.3 \text{\AA}^{-1}$ , somewhat less if a softer repulsive potential is used for the reference system. In the case of Al the behaviour is about the same but much less pronounced. In fact, the reference system describes the experimental  $S(Q)$  rather well even at small  $Q$ , which may be due to the high density of Al (Table IV). The results for Al may therefore be more uncertain. The differences between the reference systems, observed for Al and Pb, are compensated for by a suitable choice of  $C_i$ , giving the perturbation potentials  $v_1^*(r)$  shown in the figures. The agreement between the calculated  $S(Q)$  according to the Gaskell theory and the measured  $S(Q)$  is satisfactory, the latter ones being represented by the parabolic function discussed above (dots). It is also seen that when the reference system  $v_0^*(r)$  is made softer the effects on  $v_1^*(r)$  is that the minimum becomes deeper for both type I and II potentials, an effect particularly clear for Pb (Figure 3). The main difference between the type I and II potential shapes is that in the latter case the positive

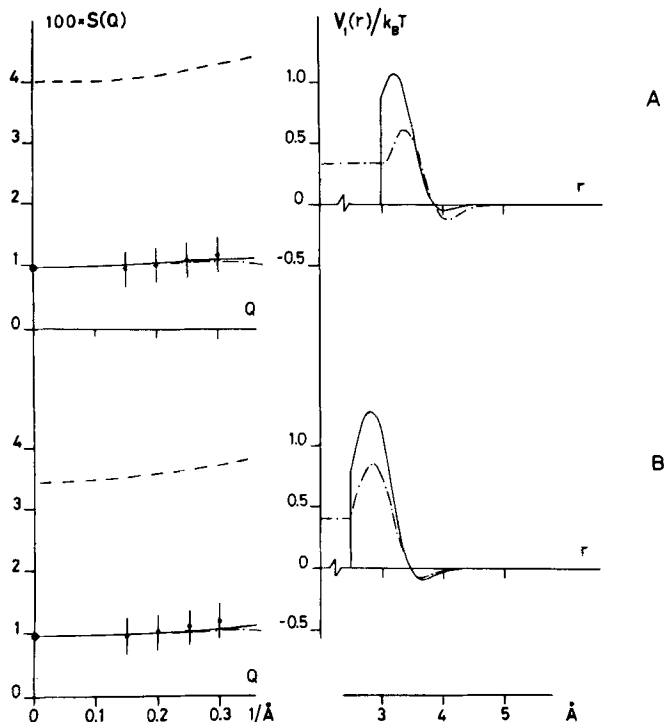


FIGURE 4 The perturbation potential  $v_1^*(r)$  and the corresponding  $S(Q)$  for liquid Bi at  $305^\circ\text{C}$ . In Figures 4A the results for an ordinary hard-core system are shown and in Figures 4B the ones due to a double-shell hard-core model (see further the text). The denotations are similar to the ones in Figures 2 and 3.

amplitude of  $v_1^*(r)$  has increased, most evident for Al (Figure 2). The observed differences between the tried "limiting cases" are considerable. It is obvious that in order to get a more accurate information about the coarse structure of the perturbation potential,  $v_0^*(r)$  must be known to a very good accuracy as well as the behaviour of  $v_1^*(r)$  for  $r < \sigma$ .

For liquid Bi two different hard-core systems were considered, the ordinary hard-core model and a double-shell model<sup>13</sup> (Table V), because the reproduction of the principal maximum with the former model was not satisfactory even with the hard-core diameter  $\sigma$  as a free parameter. The double-shell system is constructed in order to describe the anomaly of the main peak of  $S(Q)$  and implies that one assumes the existence of two different types of Bi atoms in the melt. From the Figures, 4A and B it can be seen that the two corresponding  $S_0(Q)$  differ about 20% but both of them disagrees with the measured  $S(Q)$  by a factor 3 to 4. It should also be mentioned that the two-shell model, using Orton's parameters,<sup>13</sup> describes the principal

maximum of  $S(Q)$  for Bi very good. The perturbation potential  $v_1^*(r)$  exhibits no significant difference for the two reference systems except that the amplitudes are smaller for the double-shell model. Contrary to Al and Pb the type II potential for Bi has a smaller amplitude than the type I. It is, however, obvious that  $v_1^*(r)$  in liquid Bi is quite different from that in liquid Pb. The very special shape of  $v_1^*(r)$  in the case of Bi is a direct consequence of the unusually large discrepancies between  $S_0(Q)$  and  $S(Q)$  at small  $Q$ . As it is obtained from two widely different hard-core reference systems, it most probably has same main features as a  $v_1^*(r)$  representative for the real liquid. Softer repulsive forces are certainly more realistic and may cause minor changes of the corresponding  $v_1^*(r)$  regarding the results on liquid Al and Pb. We are, however, confident that the difference between a softer reference system and the measured  $S(Q)$  would still be much larger for Bi than observed in the case of Pb or Al.

It should also be emphasized that from pure numerical reasons a monotonically decreasing and positive function for  $v_1^*(r)$  would probably also give a correct  $S(Q)$  for small  $Q$ , compare Figure 1A. Such shape has, however, been discarded on physical grounds.

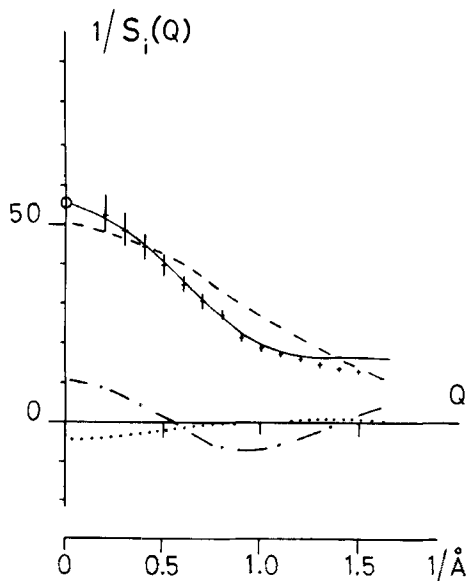


FIGURE 5 The various terms  $1/S_i(Q)$  contributing to the structure factor according to Gaskell's theory for liquid Al at  $705^\circ\text{C}$  (Eq. (2) in the text). The following denotations are used: vertical bars are measured  $1/S(Q)$ , solid line the computed  $1/S(Q)$  and broken line the reference system  $1/S_0(Q)$ —based on a  $r^{-12}$ —potential. The terms  $1/S_1(Q)$  and  $1/S_2(Q)$  are given by the dash-dotted line and by the dotted curve, respectively.  $1/S(Q)$  is thus equal to the sum of the three terms  $1/S_i(Q)$ .

### C. Comparison of the Components Entering the Calculated $S(Q)$

One example of the various contributions  $1/S_i(Q)$ , defined by Eq. (2), is plotted in Figure 5 for Al and in Figures 6A and B for Pb and Bi, respectively. The reference systems  $S_0(Q)$  for Al and Pb are based on the  $r^{-12}$  repulsive potential, while in the case of Bi the two-shell hard-core model was selected. It is seen that the term  $1/S_2(Q)$  (dotted curves) is of little importance except for Al. It is interesting to note that Gaskell's model, reproducing the measured  $1/S(Q)$  very well for small  $Q$ , starts to oscillate for  $Q > 0.5 \text{ \AA}^{-1}$  simultaneously as the reference system starts to describe the experimental values fairly well. It must, however, be pointed out that similar plots can be obtained for other reference systems. The contributory terms are then somewhat different but the final fits will be equally good. It is also worth noticing the different magnitudes of the term  $1/S_1(Q)$  for Pb and Bi, again indicating that the perturbation parts  $v_1^*(r)$  are very different for these two liquid metals. There is, furthermore, a small region in  $Q$  within which neither the Gaskell expression nor the reference system describes the measured data, particular clear for Al. This window widens when the range of  $v_1^*(r)$  increases, an effect mainly reflected in the term  $1/S_1(Q)$ .

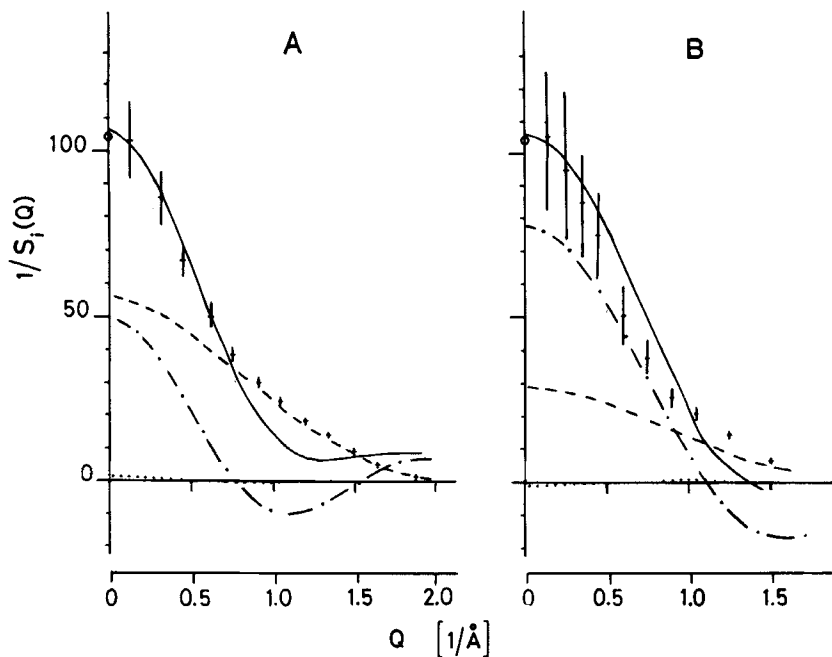


FIGURE 6 The various terms  $1/S_i(Q)$  contributing to the structure factor for liquid Pb at  $350^\circ\text{C}$  (Figure A) and for liquid Bi at  $305^\circ\text{C}$  (Figure B). The reference system for Bi is the double-shell hard-core model. Notations are the same as in Figure 5.

#### IV CONCLUSIONS

The object of the present studies of  $S(Q)$  at small  $Q$  was to establish the coarse structure of the attractive part of the effective pair-potential (or the perturbation part to a given reference potential) for liquid Al, Pb and Bi. It was found that for Al and Pb this part of the potential is of simple oscillatory nature while for Bi it is of ledge type. Thus the shoulder of the large  $Q$  side of the main diffraction peak for Bi can be related to a particular shape of an effective pair-potential. Such a relation was earlier suggested for another semi-metal, gallium.<sup>14</sup> It was further concluded that finer details in the shape of the perturbation potential cannot be uniquely revealed in the present way of analysing the experimental data. Small oscillations superimposed on the potential may very well exist but cannot be verified, because their effects on  $S(Q)$  at small  $Q$  are too small. Oscillations occurring at larger  $r$  give, if their amplitudes are not small, rise to numerical instabilities in the calculations. In such cases the periodicity of the oscillations is probably of great importance.

Concerning the coarse structure of the perturbation potential we have particularly studied two obstacles that make a more accurate analysis difficult:

- 1) The shape of the perturbation at small  $r$ , i.e. inside the range of the repulsive forces, has a clear effect on the results. The amplitude of the oscillation of the perturbation increases in going from the type I to the type II case. Differences of the order of 30% are indicated, when we try to compensate for this in order to obtain a correct small  $Q$ -behaviour of the calculated  $S(Q)$ . This ambiguity might be resolved by applying the optimized random phase approximation (ORPA).<sup>15</sup> This has not been done in the present work. However, a shape of  $v_1^*(r)$  in between the two types is probably realistic in terms of the ORPA.<sup>16</sup>

- 2) The behaviour of  $S_0(Q)$  for the reference system at small  $Q$  is also affecting the shape of the perturbation potential. When the repulsive forces get softer the negative parts of the perturbation increase, while the positive ones are nearly unchanged (except for Bi). As the strength of the repulsive forces are not known with any greater accuracy (say  $n = 10 \pm 3$  in  $v_0(r) \sim r^{-n}$  for Al and Pb) there will be an additional uncertainty in the amplitude of the derived perturbation potential, particularly the negative part. If the system can be classified as a hard or soft repulsive one the errors stay within 25% of the total amplitude when a correct small  $Q$ -behaviour is forced upon the calculated  $S(Q)$ .

Thus, these results indicate that if one intends to study the complete pair-potential by looking only at the corresponding  $S(Q)$  using, e.g. MD computations, it is necessary that the following three conditions are fulfilled.



- 1) The analysis must cover the entire  $Q$ -range from 0 to very large values.
- 2) The measured  $S(Q)$  must be very accurate, the greatest allowable error is a few percent (in relative scale). This must hold also for the small  $Q$  region.
- 3) The  $S(Q)$  obtained from MD data must agree with the measured one within the statistical limits of error of the calculation. Otherwise no quantitative conclusions can be drawn about the actual shape of the effective pair-potential.

At present the MD calculations must be performed using the trial-and-error method, because sufficiently accurate information about the pair-potential is lacking. Such a procedure will thus be very tedious. An alternative approach would be to make use of the dynamical information about the systems in question. MD studies of the pair-distribution function and the diffusion coefficient for given repulsive forces and different attractive ones have shown that the diffusion coefficient varies considerably with the shape of the attractive part of the pair-potential, while the pair-distribution functions is changing only little.<sup>17</sup> This implies that the self-motion of the particles is of main interest. This is also reflected in the dynamical structure factors although in a more involved way. The combination of structural and dynamical information is probably a more fruitful approach, as we will always face experimental data with a limited accuracy. The ability of a certain pair-potential to reproduce the measured  $S(Q)$ , within the limits of error, by— for instance—MD computations is a necessary condition, but not sufficient. The dynamics of the computer simulated system must agree with the corresponding measured data equally well.

## References

1. J. P. Hansen and D. Schiff, *Mol. Phys.*, **25**, 1281 (1973).
2. J. A. Barker and D. Henderson, *Rev. Mod. Phys.*, **48**, 587 (1976).
3. Y. Rosenfeld and N. W. Ashcroft, *Phys. Rev.*, **A20**, 1208 (1979).
4. T. Gaskell, *Phys. Lett.*, **65A**, 421 (1978).
5. R. Evans and W. Schirmacher, *J. Phys.*, **C11**, 2437 (1978).
6. U. Dahlborg and L. G. Olsson, *J. Phys.*, **41**, C8-214 (1980).
7. L. Verlet and J. J. Weiss, *Phys. Rev.*, **A5**, 939 (1972).
8. R. V. Gopala Rao and B. M. Satpathy, *Phys. Lett.*, **75A**, 220 (1979).
9. T. E. Faber, *An Introduction to the Theory of Liquid Metals*, Cambridge University Press 1972.
10. H. Ruppersberg and H. Wehr, *Phys. L.*, **40A**, 31 (1972).
11. U. Dahlborg, M. Davidovic, and K. E. Larsson, *Phys. Chem. Liq.*, **6**, 149 (1977).
12. D. M. North, J. E. Enderby, and P. A. Egelstaff, *J. Phys.*, **C1**, 1075 (1968).
13. B. R. Orton, *Z. Naturforsch.*, **34a**, 1547 (1979).
14. K. K. Mon, N. W. Ashcroft, and G. V. Chester, *Phys. Rev.*, **B19**, 5103 (1979).
15. H. C. Andersen, D. Chandler, and J. Weeks, *Advances in Chemical Physics*, **34**, 105, Wiley and Sons, 1976.
16. U. Dahlborg, unpublished.
17. T. Kinell and I. Ebbsjö, *J. Phys.*, **41**, C8-301 (1980).